

# Cooper minima and Young-type interferences in the photoionization of $\text{H}_2^+$

R. Della Picca,<sup>1,2</sup> P. D. Fainstein,<sup>1</sup> and A. Dubois<sup>2,3</sup>

<sup>1</sup>*CONICET and Centro Atómico Bariloche, Comisión Nacional de Energía Atómica, Avda E. Bustillo 9500, 8400 Bariloche, Argentina*

<sup>2</sup>*UPMC Univ. Paris 6, UMR 7614, Laboratoire de Chimie Physique-Matière et Rayonnement, 11 rue Pierre et Marie Curie, F-75231 Paris Cedex 05, France*

<sup>3</sup>*CNRS UMR 7614, LCPMR, F-75005 Paris, France*

(Received 8 June 2011; published 9 September 2011)

We present a detailed study of the partial and total cross sections for photon-induced electron emission from  $\text{H}_2^+$ . By comparing the results employing exact and approximate, bounded and continuum wave functions, for one- and two-center basis functions, we find the origin and position of the Cooper-like minima in the partial cross sections and their relationship with the Young-type interference pattern.

DOI: [10.1103/PhysRevA.84.033405](https://doi.org/10.1103/PhysRevA.84.033405)

PACS number(s): 33.80.Eh, 33.60.+q

## I. INTRODUCTION

The original Young two-slit light diffraction and interference experiment [1] established the wave nature of light. More than a hundred years later, the same kind of experiment was carried out with electrons [2–4], confirming that they also behave as waves.

The same kind of interference phenomena can be observed in the ionization of diatomic molecules, where the process is called Young-type interference, since it involves only the emission from two atomic centers without electronic wave diffraction.

For photon-impact ionization of the ground state of  $\text{H}_2^+$ , Cohen and Fano [5] showed that the total cross section is modulated by an oscillating function that gives rise to the interference pattern. Employing approximate wave functions, they found that the total cross section can be written as

$$\sigma_{\text{tot}}^{\text{CF}} = \frac{\sigma_{\text{H}}}{1+S} \left( 1 + \frac{\sin(kR)}{kR} \right), \quad (1)$$

where  $k$  is the electron momentum,  $R$  is the internuclear distance between the nuclei,  $\sigma_{\text{H}}$  is the total photoionization cross section for an equivalent H atom, and  $S$  is the overlap integral arising from the normalization of the initial wave function.

For ion impact on  $\text{H}_2$ , Young-type interferences have been observed experimentally in the electron emission spectra and interpreted as due to the sum of coherent waves emitted from each center of the molecule [6].

In a recent paper [7], the photoionization of  $\text{H}_2$  and  $\text{H}_2^+$  was investigated for photon wavelengths comparable or smaller than the internuclear distance. The total cross sections as a function of photon energy for different partial waves show distinct minima for values of the photoelectron momentum  $k$  given by

$$kR \simeq \ell\pi, \quad (2)$$

where  $R$  is the internuclear distance and  $\ell$  the partial wave quantum number. This only occurs for parallel alignment of the molecular axis with respect to the polarization vector. As this formula describes momentum quantization in a box of length  $R$ , these authors suggested that the minima in the spectra can be related to electron confinement at the given value of  $R$ .

Della Picca *et al.* [8] also studied these structures and showed that for an initial  $1s\sigma_g$  state the minima in the partial cross section correspond to maxima in the phase shift of the continuum wave  $k\ell\sigma_u$  and the transition matrix element is exactly zero. This fact suggests that the effect is similar to the Ramsauer-Townsend effect in elastic electron-atom collisions [9], which can be explained in terms of one-dimension resonance for an incident electron wave on a potential well of width  $R$ . When the well size coincides with an integer number of times of half electron de Broglie wavelength (or equivalently  $kR = n\pi$ ), a resonance occurs and the well is transparent to the electron wave [10,11].

The minima in the partial cross sections are similar to the Cooper minima appearing in atomic photoionization of states which have at least one node [12]. Since the ground states of  $\text{H}_2$  and  $\text{H}_2^+$  molecules have no nodes, it was suggested that it is due to the nonspherical character of the molecular potential [8,13] and the minima were therefore called “Cooper-like minima”. Della Picca *et al.* [8] found that these minima occur in a wide range of  $k$  and  $R$  values satisfying only approximately the relation (2) and they remain when the vibrational degree of freedom of the target is taken into account. In the following, we omit the term *like* to denote the Cooper-like minima.

In a more recent work, Della Picca *et al.* [14] showed that the Cohen and Fano oscillations due to interference effects are related to the Cooper minima. It results therefore in that the interpretation of the oscillations can be done equivalently with these two different pictures. However, the relationship between these two aspects was only investigated by comparison (i) of the minima position in the cross-section ratio and in the partial cross sections (see Fig. 4 of [14]), (ii) with the heteronuclear molecule  $\text{HeH}^{2+}$  case where the oscillations almost disappear, and (iii) with ion-impact-induced ionization (cf. also [15,16]).

The purpose of this work is to study in more detail the nature of the Cooper minima and their relationship with Young-type interferences. In Sec. II, we present the theoretical framework and in Sec. III we analyze the molecular photoionization of  $\text{H}_2^+$  using various approximations for the wave functions to allow the calculation of the partial cross sections in closed analytical form. We consider spherical (one-center basis functions) and spheroidal partial waves (two-center basis functions). In Sec. III A, we show that with the spherical waves

the exact position of the Cooper minima can be obtained and related with the interference factor  $1 + \sin(kR)/kR$ . In Sec. III B, we show that with spheroidal waves we can deduce the minima position from the interference oscillations in the cross-section ratio and obtain an expression similar to Eq. (2). Finally, in Sec. IV, we analyze the exact case and compare with results obtained in the previous sections.

Atomic units will be used except when otherwise stated.

## II. THEORY

We consider the photoionization of  $\text{H}_2^+$  by linearly polarized light from the  $1s\sigma_g$  ground state within the Born-Oppenheimer approximation. The nuclei of the molecule have charge  $Z_A = Z_B = 1$  and are fixed at the internuclear distance  $R = 2$  a.u. The differential cross sections are obtained in the dipolar approximation as a function of the photoelectron energy and angle,

$$\frac{d\sigma}{d\mathbf{k} d\Omega_R} = (2\pi)^2 \alpha \omega k |T_{if}|^2 \Big|_{E=E_i+\hbar\omega}, \quad (3)$$

where  $\mathbf{k} \equiv \{k, \theta_e, \phi_e\}$  ( $\hat{k} = \mathbf{k}/k$ ) is the ejected electron momentum in the molecular frame,  $\Omega_R \equiv \{\theta_R, \varphi_R\}$  is the orientation of the molecule in the laboratory reference frame (defined with  $\hat{z}$  axis parallel to the radiation field),  $\alpha$  is the fine-structure constant,  $\hbar\omega$  is the photon energy, and the transition matrix  $T_{if}$  is given by

$$T_{if} = \langle \Phi_f^-(\mathbf{k}, \mathbf{r}) | \hat{\varepsilon} \cdot \mathbf{D} | \Phi_i(\mathbf{r}) \rangle. \quad (4)$$

The dipole operator  $\mathbf{D}$  in Eq. (4) is given by  $\mathbf{D} = \nabla/\omega$  or  $\mathbf{D} = \mathbf{r}$  in the velocity and length gauges, respectively. The electronic functions  $\Phi_i(\mathbf{r})$  and  $\Phi_f^-(\mathbf{k}, \mathbf{r})$  are the initial and final exact wave functions with correct asymptotic conditions for the latter. Both are eigenfunctions of the electronic Hamiltonian,

$$H = -\frac{1}{2}\nabla_r^2 - \frac{Z_A}{r_A} - \frac{Z_B}{r_B}, \quad (5)$$

with eigenvalues  $E_i < 0$  and  $E = k^2/2$ , respectively.

The electronic Hamiltonian (5) commutes with the operators  $L_z$  and  $\Omega$  associated with constants of motion and related to the cylindrical symmetry of the molecule.  $L_z$  is the component along the molecular axis of the total electronic orbital angular momentum  $\mathbf{L}$ , with eigenvalue  $m\hbar$ . The operator  $\Omega$  is related to the Runge-Lenz vector and is given by [17]

$$\Omega = \mathbf{L}^2 + \frac{R^2}{4} \left( \nabla^2 - \frac{\partial^2}{\partial z^2} \right) + R(Z_A \cos \theta_A - Z_B \cos \theta_B), \quad (6)$$

where  $\theta_A$  and  $\theta_B$  are related to the angles of the electron position vector with respect to the nuclei  $A$  and  $B$ , respectively. The eigenvalues of  $\Omega$  are numbered by the quantum number  $\ell$ . As  $L_z$  and  $\Omega$  commute, the set of observables  $H$ ,  $\Omega$ , and  $L_z$  forms a complete set of commuting observables, and the eigenfunctions  $\Phi_s$  with  $s \equiv E, \ell, m$  form a basis of the Hilbert space. Since these basis functions take into account explicitly the symmetry of the molecule, we call it a ‘‘two-center’’ (2C) basis and it is given by functions of the form

$$\Phi_s(\mathbf{r}) = J_{E\ell m}(\xi) \mathcal{Y}_{E\ell m}(\eta, \varphi), \quad (7)$$

where  $(\xi, \eta, \varphi)$  are the spheroidal coordinates of the position vector  $\mathbf{r}$  and  $\mathcal{Y}_{E\ell m}$  are the spheroidal harmonics.

A different representation can be obtained employing the ‘‘one-center’’ (1C) basis that corresponds to the set of functions  $\Phi_p$  with  $p \equiv q, L, m$ , which are eigenfunctions of  $\mathbf{L}^2$ ,  $L_z$  with eigenvalues  $L(L+1)\hbar^2$  and  $m\hbar$ , respectively. In this case,  $\mathbf{L}^2$  does not commute with  $H$  and the basis wave functions can be written as the product of spherical harmonics and radial functions numbered by  $q$ ,

$$\Phi_p(\mathbf{r}) = f_q(r) Y_{Lm}(\theta, \varphi), \quad (8)$$

where  $(r, \theta, \varphi)$  are the usual spherical coordinates. In the united atom limit, the operators  $\Omega$  and  $\mathbf{L}^2$  coincide, the spheroidal harmonics become the spherical harmonics, and both bases are equal.

The continuum wave function with well-defined momentum  $\Phi_f^-(\mathbf{k}, \mathbf{r})$  can be written as the sum, with appropriate coefficients, over the index  $m$  and  $\ell$  of the elements of the 2C basis,

$$\Phi_f^-(\mathbf{k}, \mathbf{r}) = \sum_{m\ell} c_s^{2C}(\mathbf{k}) \Phi_s(\mathbf{r}), \quad (9)$$

or over the index  $m$ ,  $L$ , and  $q$  of the elements of the 1C basis,

$$\Phi_f^-(\mathbf{k}, \mathbf{r}) = \sum_{mLq} c_p^{1C}(\mathbf{k}) \Phi_p(\mathbf{r}), \quad (10)$$

where  $c_s^{2C}$  and  $c_p^{1C}$  are the expansion coefficients for the 2C and 1C basis functions. The transition matrix (4) can be written therefore as the sum of these (conjugated) coefficients multiplied by the partial transition matrix  $M_{\ell(L)m}$  defined as

$$M_{\ell(L)m} = \langle \Phi_{s(p)}(\mathbf{r}) | \hat{\varepsilon} \cdot \mathbf{D} | \Phi_i(\mathbf{r}) \rangle, \quad (11)$$

which depends on the molecular orientation.

The selection rules  $\Delta m = 0, \pm 1$  are independent of the basis, since the basis functions  $\Phi_s$  and  $\Phi_p$  have the same azimuthal dependence  $e^{im\varphi}$ . In the case of initial states with zero angular momentum ( $\sigma$  states), we can make the integration over the azimuthal angle  $\varphi$  in Eq. (11) and obtain

$$M_{Jm} = \cos \theta_R \delta_{m0} \frac{1}{\omega} \mathcal{M}_{J0} + \sin \theta_R (\delta_{m1} - \delta_{m-1}) \frac{1}{2\omega} \mathcal{M}_{J1}, \quad (12)$$

with  $J \equiv \ell$  or  $L$  and  $\delta_{mn}$  is the Kronecker's delta. The reduced transition matrix elements  $\mathcal{M}_{Jm}$  only involve integrals over the variables  $(\xi, \eta)$  or  $(r, \theta)$ . Moreover, due to the symmetry of the homonuclear molecule and the parity of the initial state, only odd  $J$  values give nonzero values of the transition matrix. The square module of the transition matrix (11) defines the partial cross section depending on the molecular orientation,

$$\frac{d\sigma_{Jm}}{d\Omega_R} = (2\pi)^2 \alpha \omega |M_{Jm}|^2. \quad (13)$$

To obtain the total cross section, we have to average over the molecular orientation and sum over all partial contributions

with  $m = 0, \pm 1$  and odd  $J$ . Then  $\sigma_{\text{tot}}$  is dependent only on the reduced transition matrices,

$$\sigma_{\text{tot}} = \frac{1}{4\pi} \int d\Omega_R \sum_{J,m=0,\pm 1} \frac{d\sigma_{Jm}}{d\Omega_R} \quad (14)$$

$$= \frac{(2\pi)^2 \alpha}{3\omega} \sum_J (|\mathcal{M}_{J0}|^2 + |\mathcal{M}_{J1}|^2), \quad (15)$$

or, equivalently,

$$\sigma_{\text{tot}} = \sum_J (\sigma_{J0} + \sigma_{J1}), \quad (16)$$

where we have introduced the partial cross sections (PCS) as

$$\sigma_{J\Lambda} = \frac{(2\pi)^2 \alpha}{3\omega} |\mathcal{M}_{J\Lambda}|^2, \quad (17)$$

defined only with  $\Lambda \equiv |m| = 0$  or  $1$ . While the PCS (17) depends on the chosen basis, the total cross section does not when convergence is obtained and therefore we have

$$\sigma_\sigma = \sum_\ell \sigma_{\ell 0} = \sum_L \sigma_{L0}, \quad (18)$$

$$\sigma_\pi = \sum_\ell \sigma_{\ell 1} = \sum_L \sigma_{L1}, \quad (19)$$

and

$$\sigma_{\text{tot}} = \sigma_\sigma + \sigma_\pi. \quad (20)$$

Note that the PCS  $\sigma_{J\Lambda}$  defined in Eq. (17) with  $\Lambda = 1$  corresponds to the sum of the  $m = 1$  and  $m = -1$  contributions and therefore a factor 2 should not be added to  $\sigma_\pi$  in Eq. (20) to obtain the total cross section. In the following sections, we discuss the properties of one- and two-center partial cross sections.

### III. ANALYSIS WITH THE LCAO-PW APPROXIMATIONS

The exact calculation of the differential and total cross sections can only be done numerically. To gain further insight, it is most convenient to obtain them in closed analytical form, which is only possible when using approximate wave functions. For this purpose, we consider the initial ground state as the simplest linear combination of atomic orbitals (LCAO),

$$\begin{aligned} \Phi_i(\mathbf{r}) &= \frac{1}{\sqrt{2(1+S)}} [\Phi_{1s}^\mu(r_A) + \Phi_{1s}^\mu(r_B)] \\ &= N \exp\left(-\frac{\mu R}{2}\xi\right) \cosh\left(\frac{\mu R}{2}\eta\right), \end{aligned} \quad (21)$$

where  $\Phi_{1s}^\mu(r) = e^{-\mu r} \sqrt{\mu^3/\pi}$  with  $\mu = 1.24$ ,  $N^2 = 2\mu^3/\pi(1+S)$ , and  $S$  is the overlap integral [18]. For the final state, we consider the plane wave (PW) approximation, which is obtained by setting  $Z_A = Z_B = 0$  in Eq. (5); in this case,  $H$  commutes with  $\mathbf{L}^2$ . The PW approximation can be written using the 1C basis representation,

$$\frac{e^{i\mathbf{k}\cdot\mathbf{r}}}{(2\pi)^{3/2}} = \frac{4\pi}{(2\pi)^{3/2}} \sum_{Lm} i^L j_L(kr) Y_{Lm}^*(\Omega_k) Y_{Lm}(\Omega), \quad (22)$$

or the 2C basis representation [19],

$$\begin{aligned} \frac{e^{i\mathbf{k}\cdot\mathbf{r}}}{(2\pi)^{3/2}} &= \frac{1}{\sqrt{k}} \sum_{m=-\infty}^{\infty} \sum_{\ell=|m|}^{\infty} i^\ell J_{\ell m}(c, \xi) \\ &\quad \times \mathcal{Y}_{\ell m}^*(c, \cos\theta_k, \varphi_k) \mathcal{Y}_{\ell m}(c, \eta, \varphi), \end{aligned} \quad (23)$$

where  $c = kR/2$ . We can identify the 1C (or spherical) partial waves as

$$\Phi_p(\mathbf{r}) = j_L(kr) Y_{Lm}(\Omega) \sqrt{\frac{2k}{\pi}} \quad (24)$$

and the 2C (or spheroidal) partial waves as

$$\Phi_s(\mathbf{r}) = \mathcal{Y}_{\ell m}(c, \eta, \varphi) J_{\ell m}(c, \xi). \quad (25)$$

With these approximations to the initial and final wave functions, gauge invariance is lost and thus the results employing the velocity or length gauge are different. In this section, we use the velocity gauge ( $\mathbf{D} = \nabla/\omega$ ) but, as discussed in the following, our conclusions on the position of the Cooper minima will be preserved in length gauge.

#### A. Calculation employing the 1C basis

In this section, we calculate the transition matrix (11) employing the wave functions (21) and (24). Since the initial LCAO state is the sum of two terms, the transition matrix can be separated into two contributions. In what follows, it will be convenient to expand the spherical partial waves  $\Phi_p$  in partial waves centered on each nucleus. This can be done through a translation of  $\pm R/2$  along the molecular axis, so they can be written as linear combinations of one-center partial waves but evaluated on each nucleus [5,20]. Thus both terms of the transition matrix are integrals over the variables  $r_A$  and  $r_B$  and are therefore proportional. The transition matrix can then be factorized as

$$M_{Lm}^{1C} = \frac{[1 - (-1)^L]}{\sqrt{2(1+S)}} T_{1L}^{(m)*}(kR/2) M_{1m}^{\text{atom}}, \quad (26)$$

where the translation operators  $T_{1L}^{(m)}$  are proportional to the spherical Bessel functions and their first derivative

$$T_{1L}^{(0)}(c) = \sqrt{3(2L+1)} j_L'(c), \quad (27)$$

$$T_{1L}^{(\pm 1)}(c) = \sqrt{\frac{3L(L+1)(2L+1)}{2}} \frac{j_L(c)}{c}, \quad (28)$$

and

$$\begin{aligned} M_{1m}^{\text{atom}} &= \langle \Phi_{p=1,m}(\mathbf{r}) | \hat{\varepsilon} \cdot \mathbf{D} | \Phi_{1s}^\mu(r) \rangle = -\tilde{\Phi}_{1s}(k) \frac{k^{3/2}}{\omega} \sqrt{\frac{2\pi}{3}} \\ &\quad \times [\sqrt{2} \cos\theta_R \delta_{m0} + \sin\theta_R (\delta_{m1} - \delta_{m-1})]. \end{aligned} \quad (29)$$

Finally, averaging the square modulus of the transition matrix over molecular orientation we obtain the PCS,

$$\sigma_{L0}^{1C} = \frac{\sigma_H}{1+S} \frac{2}{3} |T_{1L}^{(0)}(kR/2)|^2 \quad (30)$$

and

$$\sigma_{L1}^{1C} = \frac{\sigma_H}{1+S} \frac{4}{3} |T_{1L}^{(1)}(kR/2)|^2, \quad (31)$$

where

$$\sigma_H = (2\pi)^3 \frac{2\alpha}{3\omega} k^3 \tilde{\Phi}_{1s}^2. \quad (32)$$

From the properties of the spherical Bessel functions, Cohen and Fano [5] showed that the sum of the translation operators over odd  $L$  and  $m = 0, \pm 1$  gives the interference term

$$\frac{2}{3} \sum_{L,m=0,\pm 1} |T_{1L}^{(m)}(kR/2)|^2 = \left[ 1 + \frac{\sin(kR)}{kR} \right]. \quad (33)$$

Finally, with this expression, they summed the PCS (30) and (31) obtaining their Eq. (1), which showed for the first time the interference effect.

The Cooper minima (zeros of the transition matrix) are the zeros of the translation operators [21]. Therefore, they are directly related to the molecular structure and occur when the spherical Bessel function ( $|m| = 1$  case) or their first derivative ( $m = 0$  case) are zero. Moreover, Eq. (33) establishes the relationship between the Cooper minima and Young-type interference: the zeros of the spherical Bessel functions and their derivatives give the oscillatory feature of the PCS and when these terms are summed the interference pattern is obtained.

In Fig. 1, we present the 1C PCS as function of the electronic momentum for different odd values of  $L$  and  $\Lambda = 0, 1$ . According to Eqs. (30) and (31), they correspond to a monotonically decreasing atomic cross section multiplied by the translation operators that are proportional to the spherical Bessel functions or their derivatives. In Fig. 1, the zeros of  $j_L$  and  $j'_L$  appear as deep minima and one can observe, for example, that  $\sigma_{10}^{1C}$  have Cooper minima when  $kR/2 = 2.08, 5.94, 9.2, \dots$ , which are the zeros of  $j'_1$ . Finally, when we sum all the PCS, we obtain the total cross section  $\sigma_{\text{tot}}$ , which when divided by the atomic total cross section  $\sigma_H$  gives the ratio plotted in the lower panel.

From Figs. 1(a) and 1(b), it is not straightforward to observe that the PCS oscillations give rise to the oscillatory behavior of the cross section ratio in Fig. 1(c). However, it is easy to understand analytically from Eq. (33).

### B. Calculation employing the 2C basis

In this section, we calculate the PCS employing the 2C basis functions. This is done numerically in the same way as described in our previous works [8,14], but setting  $Z_A = Z_B = 0$  to obtain the PW approximation. We evaluate Eq. (11) with the wave functions (21) and (25).

The results are presented in Fig. 2:  $\sigma_{\ell 0}$  in the upper panel and  $\sigma_{\ell 1}$  in the lower one. Unlike the 1C case, only the  $\Lambda = 0$  case presents structures and each PCS has a unique minimum. The sum over all PCS gives the same total cross section as in the 1C case, and the interference function  $1 + \sin(kR)/kR$  is obtained again after division by the atomic total cross section  $\sigma_H$  [shown in Fig. 1(c)].

To understand the differences between the structures in the PCS obtained with the 1C and 2C basis, it is convenient to analyze both transition matrices. In the Appendix, we show

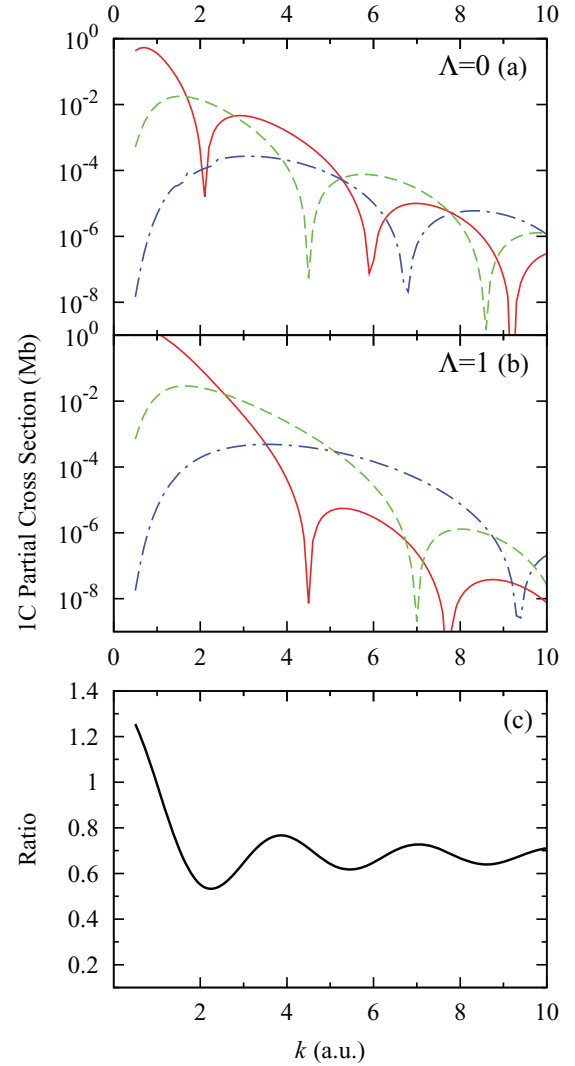


FIG. 1. (Color online) 1C partial cross sections  $\sigma_{Lm}^{1C}$  using LCAO and PW with  $L = 1$  solid (red),  $L = 3$  dashed (green), and  $L = 5$  dashed dotted (blue) lines. (a)  $\Lambda = 0$  case. (b)  $\Lambda = 1$  case. (c) Molecular and atomic total cross-section ratio.

that the 2C transition matrix can be written as the sum of 1C transition matrices. According to Eqs. (26) and (A3), we have

$$M_{\ell 0} = \frac{2\sqrt{3}}{\sqrt{1+S}} M_{10}^{\text{atom}} \sum_{L(\text{odd})=1} (-i)^{L-\ell} d_L(c, \ell, 0) j'_L(c), \quad (34)$$

$$M_{\ell \pm 1} = \frac{2\sqrt{3}}{\sqrt{1+S}} M_{1\pm 1}^{\text{atom}} \sum_{L(\text{odd})=1} (-i)^{L-\ell} \times L(L+1) d_{L-1}(c, \ell, 1) \frac{j_L(c)}{\sqrt{2c}}. \quad (35)$$

The coefficients  $d_n(c, \ell, |m|)$  are defined in the Appendix and they relate the spheroidal and spherical harmonics. In Fig. 3, we show the most significant coefficients as a function of the parameter  $c = kR/2$ .

We begin with the  $m = 0$  case. At low energy (or small values of  $c$ ), the coefficients  $d_L(c, \ell, |m| = 0)$  are larger when  $L = \ell$ . Thus the higher contribution to the transition matrix

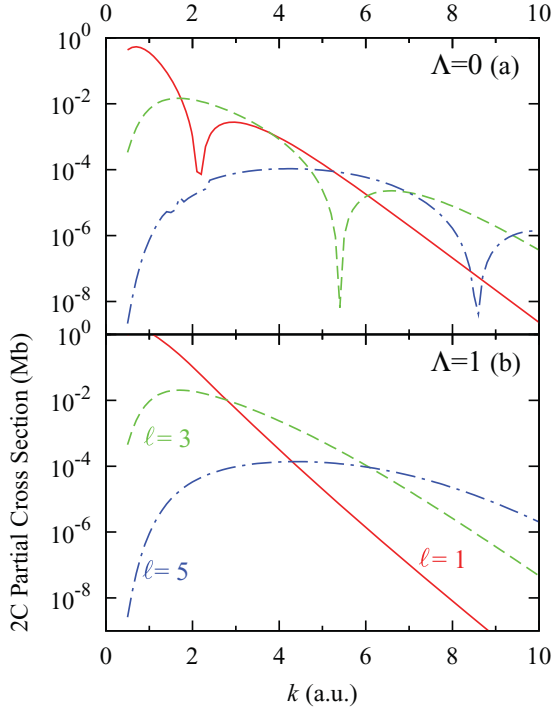


FIG. 2. (Color online) 2C partial cross sections  $\sigma_{\ell m}$  using LCAO and PW with  $\ell = 1$  solid (red),  $\ell = 3$  dashed (green), and  $\ell = 5$  dashed dotted (blue) lines. (a)  $\Lambda = 0$  case. (b)  $\Lambda = 1$  case.

is due to the  $d_{\ell}(c, \ell, 0)j'_{\ell}(c)$  term. For example, we can expect a Cooper minimum in the PCS with  $\ell = 1$  due to the zero in the derivative of the spherical Bessel function of order 1, and this happens when  $c = 2.08$ . As the energy increases, the coefficients  $d_{\ell}(c, \ell, 0)$  and  $d_{\ell+2}(c, \ell, 0)$  become of the same order and the contributions of the spherical Bessel function derivatives with orders  $\ell$  and  $\ell + 2$  are comparable. For example, the minimum in the PCS with  $\ell = 3$  at  $k = 4.9$  a.u. falls between the first zeros of  $j'_3$  and  $j'_5$ , that are 4.51 and 6.76, respectively. As  $c$  increases, more coefficients  $d_n$  become important and there are contributions from many spherical Bessel functions preventing therefore the transition matrix from vanishing for another value of energy. The  $|m| = 1$  case is quite different, as the factor  $L(L + 1)$  appears in Eq. (35), allowing the coupling of spherical Bessel functions of higher order. Many comparable terms contribute to the summation and therefore the matrix element is always nonvanishing.

Since for each  $\ell$  value the amplitudes (34) and (35) and the coefficients  $d_L$  depend on the energy only through the parameter  $c = kR/2$ , we can infer that the Cooper minima in the LCAO-PW approximation appear when  $kR \sim \beta_{\ell}$ , where  $\beta_{\ell}$  is some constant which depends only on  $\ell$  [21]. In spite of these expressions, it is not straightforward to determine the appropriate constant  $\beta_{\ell}$  for each  $\ell$  value.

With the 1C basis, we could obtain analytically the shape of the PCS and how their sum results in the interference factor. On the contrary, with the 2C basis the PCS do not have a simple analytical expression but minima can be seen graphically: the total cross section results from the sum of PCS with a unique structure in the energy range where each PCS gives the main contribution to the total cross section. This Cooper minimum

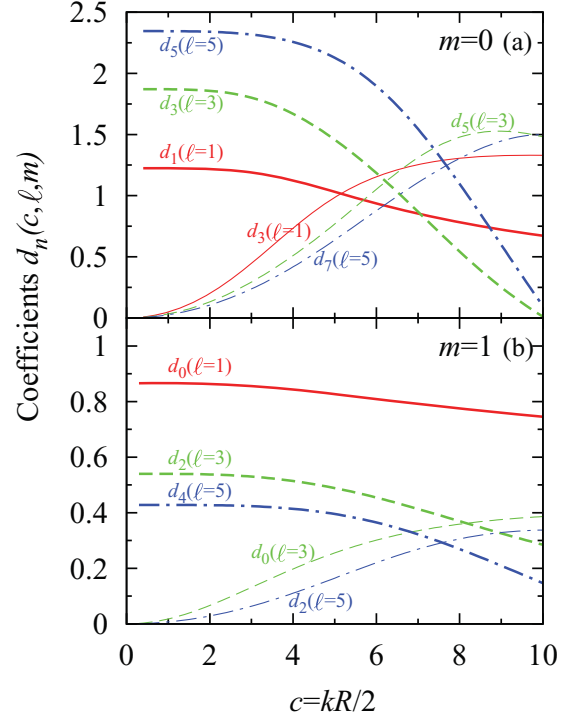


FIG. 3. (Color online) Coefficients  $d_n(c, \ell, |m|)$  as functions of the parameter  $c = kR/2$  for  $\ell = 1$  solid (red),  $\ell = 3$  dashed (green), and  $\ell = 5$  dashed dotted (blue) lines. (a)  $m = 0$  case, with coefficients  $d_{\ell}$  in thick lines and  $d_{\ell+2}$  with thin lines. (b)  $m = 1$  case, with coefficients  $d_{\ell-1}$  in thick lines and  $d_{\ell-3}$  with thin lines.

is therefore translated directly to the total cross section and then to the cross-section ratio.

Unlike the 1C case, with the 2C basis we do not obtain analytically the position of the minima. However, we know that the minima in the cross-sections ratio occur when the interference term in Eq. (1) is minimum, i.e.,  $[1 + j_0(kR)]' = 0$  with positive second derivative. Since  $j'_0 = -j_1$ , the minima occurs when  $kR$  is a zero of the first-order spherical Bessel function, with negative derivative. These zeros of  $j_1$  have values very close to those for which  $\sin(kR) = -1$  or, similarly, when  $kR = \pi(n + \frac{1}{2})$  with odd  $n$ . If we assume that each minimum of the cross-section ratio comes from the minimum in each PCS, one may conclude that the Cooper minimum of the PCS  $\sigma_{\ell 0}$  occurs when

$$kR = \pi(\ell + \frac{1}{2}) \quad (36)$$

is verified. Since the LCAO-PW approximation is expected to be valid for large values of  $k$ , Eq. (36) will be verified when  $\ell$  is large. In this case,  $\ell \simeq \ell + \frac{1}{2}$  and the result thus agrees with the qualitative findings of [7] given in Eq. (2).

#### IV. CALCULATION WITH EXACT WAVE FUNCTIONS

Finally, in this section we present 1C and 2C PCS employing exact initial and final wave functions, i.e., eigenfunctions of the Hamiltonian (5) with  $Z_A = Z_B = 1$ ; in this way, the calculations preserve gauge invariance. The ground initial and continuum final wave functions are the same as the ones we

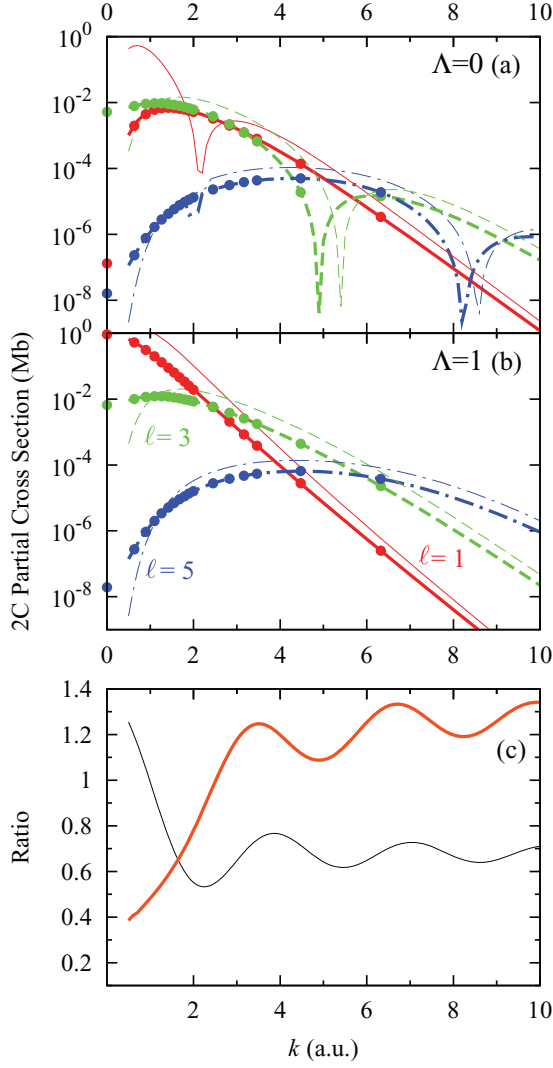


FIG. 4. (Color online) 2C PCS as in Fig. 2. Thin lines using LCAO-PW and thick lines employing exact wave functions. Dots from [22].

have used in previous works [8,14] where the 2C PCS were obtained numerically.

In Fig. 4, we show the 2C PCS with thick lines and compare with the results of the previous sections (LCAO-PW with thin lines). We also include the results of Richards and Larkins [22] with dots. In the lower panel, we show the cross-section ratio  $\sigma_{\text{tot}}^{\text{approx}}/\sigma_{\text{H}}$ , as in Figs. 1(c) and 2(c) with thin lines and  $\sigma_{\text{tot}}/\sigma_{\text{atom}}$  with thick line, where

$$\sigma_{\text{atom}} = (2\pi)^2 \frac{2\alpha}{3\omega} \frac{2^5}{(1+k^2)^3} \frac{\exp[-4/k \tan^{-1}(k)]}{1 - \exp(-2\pi/k)} \quad (37)$$

corresponds to the exact total cross section for photoionization of the ground-state hydrogen atom.

We can observe that the behavior of the *approximate* PCS (with LCAO-PW approximations) is similar to the exact ones, except for  $\ell = 1$  and energies close to 2 a.u., where the approximate case presents a Cooper minimum that appears below threshold in the exact case. This means that the approximate cross-section ratio shows an extra minimum at this energy. Moreover, the different behavior of the ratios at low

energies is due to the different denominators: in the exact case Eq. (37) and in the approximate case  $\sigma_{\text{H}}$ , defined in Eq. (32).

The evaluation of 1C PCS must be done carefully since the exact partial waves  $\Phi_p$  have not associated an eigenvalue of  $H$ . However an alternative 1C PCS can be derived: given a continuous wave function with defined momentum, we can evaluate  $T_{if}$  from Eq. (4) and express it as a sum of two-body fixed  $\sigma \rightarrow \sigma$  and  $\sigma \rightarrow \pi$  electronic dipole transition elements (see [23,24])

$$T_{if} = \cos \theta_R m_\sigma - \cos \varphi_k \sin \theta_R m_\pi, \quad (38)$$

where  $m_\sigma$  and  $m_\pi$  can be written as a series of Legendre associated functions,

$$m_\sigma = \frac{1}{\sqrt{2\pi k \omega}} \sum_L f_L^\sigma P_L^0(\cos \theta_k), \quad (39)$$

$$m_\pi = \frac{1}{\sqrt{2\pi k \omega}} \sum_L f_L^\pi P_L^1(\cos \theta_k). \quad (40)$$

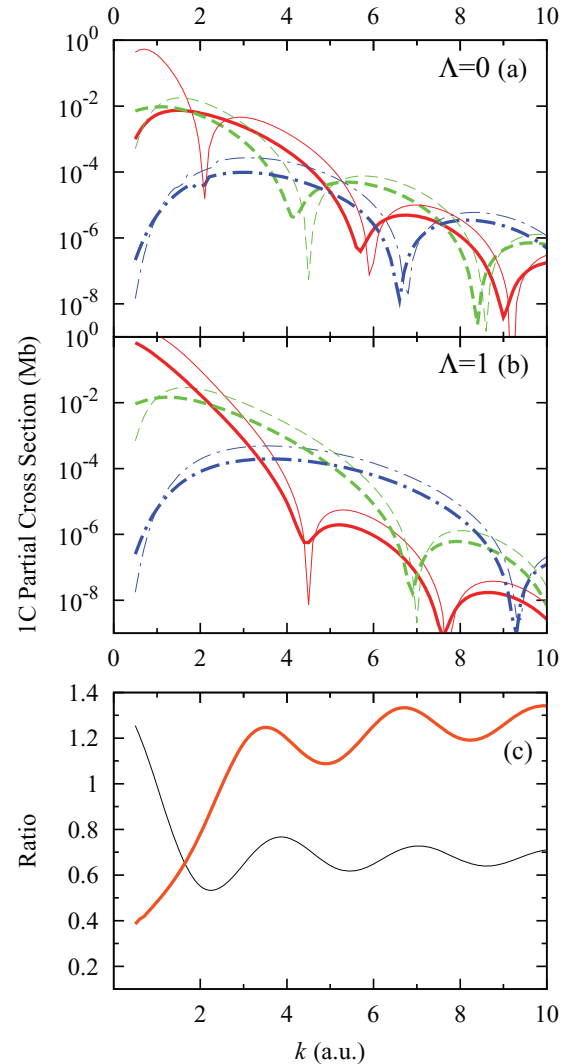


FIG. 5. (Color online) 1C PCS as in Fig. 1. Thin lines using LCAO-PW and thick lines employing exact wave functions.

Thus we can obtain the 1C PCS from the coefficients  $f_L$ ,

$$\sigma_{L0}^{1C} = (2\pi)^2 \frac{2\alpha}{3\omega} |f_L^\sigma|^2 \frac{1}{2L+1}, \quad (41)$$

$$\sigma_{L1}^{1C} = (2\pi)^2 \frac{2\alpha}{3\omega} |f_L^\pi|^2 \frac{L(L+1)}{2L+1}. \quad (42)$$

In Fig. 5, we show these PCS with thick lines, and compare with the results of the previous Sec. III A with thin lines. In the lower panel, we show the cross-section ratio as in Fig. 4(c). As in the 2C case, the exact and approximate PCS behave in the same way, except for  $L = 1$  and  $k \sim 2$ , for which there is no Cooper minima in the exact case.

In the works of Semenov *et al.* [25], Liu *et al.* [26], and Fojón *et al.* [27] for photoionization of  $N_2$  and  $H_2$ , the PCS minima are located at an energy value close to a zero of the spherical Bessel functions or their derivatives evaluated in  $c = kR/2$ . This fact is in total agreement with the analysis presented here.

Finally, we can observe from these figures that in general the *approximate* Cooper minima appear at higher energies than the exact ones. As presented previously, the minima in the approximate case should occur when Eq. (36) is satisfied. Thus the term  $1/2$  in this equation could be omitted to deduce Eq. (2), since the minima are shifted to lower energy values.

We note that this difference between the exact and approximate values of the Cooper minima position is very important in relation to recent studies of the strong-field approximation (SFA) for high-order harmonic generation from molecules by intense laser pulses. In the SFA, the corresponding yield is written in terms of the photoionization cross section, which can be employed for time-resolved dynamic chemical imaging of transient molecules. In this context, the correct calculation of these cross sections plays a critical role as highlighted in a recent comparison between SFA and exact calculations [28].

## V. CONCLUSIONS

We have studied the partial and total cross section for photoionization of  $H_2^+$ . For approximate initial wave functions and final state 1C basis functions, we find that the Cooper minima are due to the molecular or geometric structure and their position corresponds to the zeros of the spherical Bessel functions and their first derivatives. Moreover, the relationship with Young-type interference is established in an analytical expression. After carrying out a change of basis (2C basis functions), only one Cooper minima can be observed for each  $\ell$  partial cross section and only for the  $\Lambda = 0$  case. Since the position of the minima in the Young-type oscillation of the total cross-section ratio is known, we could calculate the position of the Cooper minima. Finally, we showed that the results employing exact wave functions present similar behavior with a shift in the position of the Cooper minima.

In summary, we have shown that the qualitative “confinement” rule  $kR = \ell\pi$  can be deduced from the Young-type interference pattern or the position of the Cooper minima.

## ACKNOWLEDGMENTS

R.D.P. gratefully acknowledges fruitful discussions with M. L. Martiarena. The research leading to these results has received funding from the EU Seventh Framework Programme under Grant No. PIRSES-GA-2010-269243.

## APPENDIX: RELATIONSHIP BETWEEN 1 AND 2 CENTER TRANSITION MATRIX

The spheroidal harmonics are quasiangular eigenfunctions of the Hamiltonian (5). They can be obtained as a linear combination of the spherical harmonics,

$$\mathcal{Y}_{\ell m}(c, \eta, \varphi) = \sum_{L=|m|}^{\infty} \sqrt{\frac{2(L+|m|)!}{(2L+1)(L-|m|)!}} \times d_{L-|m|}(c, \ell, |m|) Y_{Lm}(\eta, \varphi), \quad (A1)$$

where the real coefficients  $d_n$  are determined by a recurrence rule [19]. These coefficients depend on the quantum numbers  $\ell$  and  $|m|$  and depend on the energy through the parameter  $c = kR/2$ . In the homonuclear case, Eq. (A1) is the same for the plane wave and exact continuum wave function, since the quasiangular equation depends only on the difference of the nuclear charges  $Z_A - Z_B$ . In this case, we only have coefficients with even (odd)  $n$  if  $\ell - |m|$  is even (odd), respectively. In the limit  $c \rightarrow 0$ , the coefficients  $d_n(c, \ell, |m|)$  are proportional to the Kronecker's delta  $\delta_{n+|m|, \ell}$ ; thus both harmonics are the same. In Fig. 3, we show some coefficients as functions of  $c$  for  $\ell = 1, 3, 5$  and  $m = 0, 1$ . We can see that for low  $c$  the coefficient  $d_{\ell-|m|}(c, \ell, |m|)$  is larger.

To relate the 1C and 2C partial wave expansions, we utilize the expressions for the plane wave with spherical (22) and spheroidal (23) harmonics. We multiply both equations by  $\mathcal{Y}_{JM}(\Omega_k)$  and integrate over the variable  $\Omega_k$ . Employing the orthonormality condition for the spherical and spheroidal harmonics and renaming the index appropriately, we obtain

$$J_{\ell m}(c, \xi) \mathcal{Y}_{\ell m}(\eta, \varphi) = \sum_{L=|m|}^{\infty} i^{L-\ell} \sqrt{\frac{2(L+|m|)!}{(2L+1)(L-|m|)!}} \times d_{L-|m|}(c, \ell, |m|) \sqrt{\frac{2k}{\pi}} j_L(kr) Y_{Lm}(\theta, \varphi). \quad (A2)$$

Thus the 2C transition matrices (11) can be written as

$$M_{\ell m} = \sum_{L=|m|}^{\infty} (-i)^{L-\ell} \sqrt{\frac{2(L+|m|)!}{(2L+1)(L-|m|)!}} \times d_{L-|m|}(c, \ell, |m|) M_{Lm}^{1C}. \quad (A3)$$

[1] T. Young, *Phil. Trans. R. Soc. London* **94**, 1 (1804).

[2] C. Davisson and L. H. Germer, *Phys. Rev.* **30**, 705 (1927).

[3] G. P. Thomson and A. Reid, *Nature (London)* **119**, 890 (1927).

[4] C. Jönsson, *Am. J. Phys.* **42**, 4 (1974).

- [5] H. D. Cohen and U. Fano, *Phys. Rev.* **150**, 30 (1966).
- [6] N. Stolterfoht *et al.*, *Phys. Rev. Lett.* **87**, 023201 (2001).
- [7] J. Fernández, O. Fojón, A. Palacios, and F. Martín, *Phys. Rev. Lett.* **98**, 043005 (2007).
- [8] R. Della Picca, P. D. Fainstein, M. L. Martiarena, and A. Dubois, *Phys. Rev. A* **77**, 022702 (2008).
- [9] C. J. Joachain, *Quantum Collision Theory* (North-Holland, Amsterdam, 1983).
- [10] L. Schiff, *Quantum Mechanics* (McGraw-Hill, New York, 1950).
- [11] Mott and Massey, *The Theory of Atomic Collisions*, 3rd ed. (Oxford University Press, New York, 1971), Chap. 18.
- [12] J. W. Cooper, *Phys. Rev.* **128**, 681 (1962).
- [13] S. K. Semenov and N. A. Cherepkov, *J. Phys. B* **36**, 1409 (2003).
- [14] R. Della Picca, P. D. Fainstein, M. L. Martiarena, N. Sisourat, and A. Dubois, *Phys. Rev. A* **79**, 032702 (2009).
- [15] N. Sisourat, J. Caillat, A. Dubois, and P. D. Fainstein, *Phys. Rev. A* **76**, 012718 (2007).
- [16] L. Saelen, T. Birkeland, N. Sisourat, A. Dubois, and J. P. Hansen, *Phys. Rev. A* **81**, 022718 (2010).
- [17] H. A. Erikson and E. L. Hill, *Phys. Rev.* **75**, 29 (1949).
- [18] S. W. Kim, T. Y. Chang, and J. O. Hirschfelder, *J. Chem. Phys.* **43**, 1092 (1965).
- [19] P. M. Morse and H. Feshbach, *Methods of Theoretical Physics* (McGraw-Hill, New York, 1953).
- [20] M. Danos and L. C. Maximon, *J. Math. Phys.* **6**, 766 (1965).
- [21] Note that for the 1C, as well as 2C, approximate treatments of the position of the Cooper minima are gauge invariant, since the dipole operator is located in the atomic transition matrix  $M^{\text{atom}}$ .
- [22] J. A. Richards and F. P. Larkins, *J. Phys. B* **19**, 1945 (1986).
- [23] M. Walter and J. Briggs, *J. Phys. B* **32**, 2487 (1999).
- [24] R. Della Picca, P. D. Fainstein, M. L. Martiarena, and A. Dubois, *Phys. Rev. A* **75**, 032710 (2007).
- [25] S. K. Semenov, N. A. Cherepkov, M. Matsumoto, T. Hatamoto, X.-J. Liu, G. Prümper, T. Tanaka, M. Hoashino, H. Tanaka, F. Gel'mukhanov, and K. Ueda, *J. Phys. B* **39**, L261 (2006).
- [26] X.-J. Liu, N. A. Cherepkov, S. K. Semenov, V. Kimberg, F. Gel'mukhanov, G. Prümper, T. Lischke, T. Tanaka, M. Hoshino, H. Tanaka, and K. Ueda, *J. Phys. B* **39**, 4801 (2006).
- [27] O. A. Fojón, A. Palacios, J. Fernández, R. D. Rivarola, and F. Martín, *Phys. Lett. A* **350**, 371 (2006).
- [28] A.-T. Le, R. Della Picca, P. D. Fainstein, D. A. Telnov, M. Lein, and C. D. Lin, *J. Phys. B* **41**, 081002 (2008).